communications biology

A Nature Portfolio journal

Article

https://doi.org/10.1038/s42003-025-07873-8

Cd248a regulates pericyte development and viability in zebrafish

Chao Wang[1,7], Yinming Zhong[2,7], Yi Zhang[1,7], Yiyang Jiang[3], Chenshiyu Wang[1], Lele An[1], Chunhua Luo[1], Lan Yang[1,4], Zhicheng He[1], Ying Yang[1], Min Luo[1,5,6], Min Mao[1], Wenying Wang[1], Qing Liu[1], Yu Shi[1,4] ✉ & Yi-Fang Ping[1,4] ✉

CD248 is a pericyte marker during embryonic and tumor neovascularization. Although its expression pattern and function in mammalian pericytes have been extensively studied, its role in zebrafish pericytes remains largely unexplored. In this study, we identify that among the two zebrafish orthologs of human CD248, *cd248a*, rather than *cd248b*, is predominantly expressed in pericytes during embryonic development. We generate *cd248a* and *cd248b* mutant zebrafish (*cd248a*$^{cc11/cc11}$ and *cd248b*$^{cc12/cc12}$) and observe a significant reduction in pericyte numbers in *cd248a*$^{cc11/cc11}$ mutants, accompanied by disruption of the blood-brain barrier. Notably, treatment with AG1295, a platelet-derived growth factor receptor inhibitor, attenuates the increase in pericyte proliferation induced by *cd248a* overexpression. Additionally, we find that $CoCl_2$-induced pericyte apoptosis is enhanced in *cd248a*$^{cc11/cc11}$ larvae, indicating that *cd248a* provides protection against hypoxia-induced apoptosis. Taken together, our findings elucidate the role and underlying mechanisms of *cd248a* in regulating pericyte proliferation and apoptosis in zebrafish.

Pericytes, recognized as vascular mural cells embedded within the basement membrane of capillaries, play crucial roles in regulating blood flow, stabilizing capillary structures, and maintaining the integrity of the blood–brain barrier (BBB)[1,2]. The loss or dysfunction of pericytes leads to the development and progression of various diseases, such as diabetes[3,4], Alzheimer's disease[5], stroke[6], amyotrophic lateral sclerosis[7] and aging[8].

In the past decade, several analyses have revealed the basic molecular mechanisms regulating pericyte development, including PDGFRβ signaling[9], Notch signaling[10], TGFβ/BMP signaling[11] and sonic hedgehog signaling[12]. However, given the heterogeneity of pericyte transcription profiles and spatial distribution, it is necessary to identify candidate gene functions for pericyte development. This will enhance our understanding of the pathogenesis of diseases related to pericyte disorders and provide insights for future therapeutic approaches.

CD248, also known as tumor endothelial marker 1 or endosialin, is a type I single transmembrane glycoprotein. It serves as a pericyte marker during embryonic and tumor neovascularization, being highly expressed by pericytes and fibroblasts in developing embryos and tumors undergoing active physiological or pathological angiogenesis, but weakly expressed in normal adult tissues[13,14]. Both types of angiogenesis are largely induced by the hypoxic microenvironment, and further studies have confirmed that CD248 transcription is regulated by HIF-2[15]. CD248-deficient mice exhibit fully developed and functional vasculature and normal wound healing[16]. However, other studies have shown that CD248 can enhance wound healing by interacting with PDGFR[17]. Moreover, a defect in selective vessel regression leading to increased vessel density was observed in CD248 knockout mice in a postnatal retina model[18]. In contrast, tumor volume and density of vessels and pericyte density are lower in orthotopic lung cancer-transplanted mice lacking CD248[19]. These contrasting results may be related to the functional heterogeneity of CD248 in different organs. Additionally, CD248 is significantly increased in liver injury and can regulate hepatic stellate cell proliferation in response to PDGF-BB stimulation[20]. CD248 is also required for complete popliteal lymph node expansion and subsequent immune responses[21]. Recently, zebrafish-deficient models of *cd248a* and *cd248b* (orthologs of human CD248) were reported, and the expression of proinflammatory cytokines was downregulated when the zebrafish were treated with LPS in their deficient model[22].

Despite significant advancements in understanding the role of CD248 in various physiological and pathological processes, the specific role and

[1]Institute of Pathology and Southwest Cancer Center, Southwest Hospital, Third Military Medical University (Army Medical University) and Key Laboratory of Tumor Immunopathology, Ministry of Education of China, Chongqing, China. [2]School of Medicine, Chongqing University, Chongqing, China. [3]School of Basic Medical Sciences, Southern Medical University, Guangzhou, China. [4]Jinfeng Laboratory, Chongqing, China. [5]Graduate School of Guangzhou Medical University, Guangzhou, China. [6]Guangzhou Laboratory, Guangzhou International Bio Island, Guangzhou, China. [7]These authors contributed equally: Chao Wang, Yinming Zhong, Yi Zhang. ✉e-mail: shiyu@tmmu.edu.cn; pingyifang@tmmu.edu.cn

molecular mechanisms of CD248 in pericyte proliferation and survival remain undefined. The zebrafish model offers advantages in visualizing vascular development using fluorescently labeled pericyte reporter lines, providing an excellent opportunity to explore the roles of cd248 in regulating pericyte proliferation and apoptosis. In this study, we examined the expression patterns of two *cd248* paralogs (a and b) in zebrafish and generated mutants via CRISPR/Cas9 to determine whether *cd248a* or *cd248b* mutation affects pericyte proliferation and apoptosis. Our results suggest that *cd248a* deficiency reduces pericyte number by regulating Pdgfrβ function during embryonic development and increases pericyte apoptosis induced by hypoxia in zebrafish larvae. Our newly established zebrafish mutant lines and related studies will help us elucidate the molecular mechanism of the effects of the *cd248a* and *cd248b* genes on pericyte function.

Results

Temporal and spatial gene expression profiles of *cd248a* and *cd248b*

It has been reported that human CD248 is primarily expressed in developing embryos but is weakly expressed in normal adult tissues. We wondered whether the zebrafish paralogs, *cd248a* and *cd248b*, exhibit similar expression patterns. We investigated the expression levels of *cd248a* and *cd248b* at various embryonic stages and in different adult zebrafish organs using qPCR. As shown in Fig. 1a, both genes displayed almost consistent expression trends during embryonic development. Their expression levels gradually increased from 0.5 dpf to 7 dpf, with a sharp rise at 2 dpf and a slight decrease at 3 dpf. Moreover, the expression level of *cd248a* was significantly higher than that of *cd248b* at the same developmental stage. In adult fish, the expression of *cd248a* was extremely low in most organs, except for the heart and kidney, and was much lower in adult fish compared to embryos at 0.5 dpf. In contrast, *cd248b* was expressed at high levels in organs other than the ovary (Fig. 1b). To directly compare the expression levels of *cd248a* and *cd248b* in embryonic and adult organs, we performed semiquantitative RT-PCR. The results were consistent with the qPCR results (Fig. 1c).

cd248a is highly expressed in most pericytes during embryonic development

To identify the cell populations that express *cd248a* and *cd248b*, we analyzed published single-cell sequencing data from different developmental stages in zebrafish (14–120 hpf)[23]. The distributions of nonskeletal muscle subclusters were superimposed on the temporally coded UMAP (Fig. 2a). We then constructed UMAP plots of genes associated with pericytes and vascular smooth muscle cells (vaSMCs) (Fig. 2b, c, Supplementary Fig. 1). Our results showed that *cd248a* is highly expressed in pericytes, consistent with the expression of *pdgfrβ*, the most specific and reliable vascular mural cell marker. In contrast, *cd248b* is expressed in only a very small proportion of pericytes. We also found that *cd248a* correlates most highly with *pdgfrβ* (Fig. 2d) and indeed, *cd248a* is expressed in the majority of *pdgfrβ*$^{+}$ cells (Fig. 2e).

To confirm the expression of *cd248* isoforms in zebrafish pericytes, we sorted endothelial cells and pericytes via FACS from zebrafish embryos with Ki(*pdgfrβ*: Gal4) and Tg(UAS:GFP; *fli1*:DsRed) transgenic backgrounds, which expressed GFP and DsRed in pericytes and endothelial cells, respectively (Fig. 2f, g). The expression levels of *cd248a* and *cd248b* in these two distinct cell populations were analyzed via qPCR. The results revealed that both *cd248a* and *cd248b* were expressed in pericytes; but the expression of *cd248a* was higher than that of *cd248b* (Fig. 2h). Moreover, we obtained similar results by analyzing publicly available transcriptomics data comparing *pdgfrβ*$^{+}$ vs. *pdgfrβ*$^{-}$ cells[24] and *acta2*$^{+}$ vs. *acta2*$^{-}$ cells[25] in zebrafish (Supplementary Fig. 2). Taken together, these data strongly support that *cd248a* is an ideal pericyte marker gene during embryonic development.

cd248a mutant zebrafish exhibits a deficit of pericytes

To examine whether *cd248a* and *cd248b* are important for pericyte development, we employed the CRISPR/Cas9 technique to generate mutants in zebrafish. Both *cd248a* and *cd248b* consist of a single exon, and we targeted the region near the N-terminus for mutagenesis. We successfully identified and confirmed *cd248a* and *cd248b* mutants with 4 bp and 17 bp deletions, respectively, through sequence analysis (Fig. 3a-d). These mutant zebrafish lines were registered with ZFIN under the designations *cd248a*$^{cc11/cc11}$ and *cd248b*$^{cc12/cc12}$, respectively. We compared

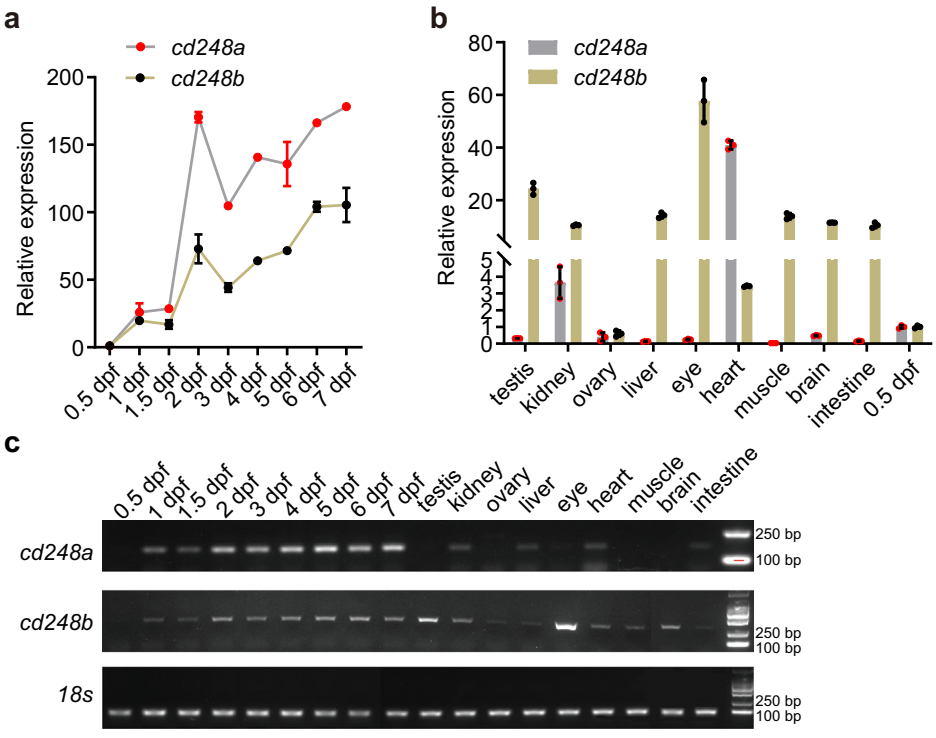

Fig. 1 | Relative temporal and spatial gene expression of *cd248a* and *cd248b*. Relative expression levels of *cd248a* and *cd248b* at different developmental stages (**a**) and in various adult zebrafish tissues (**b**). Gene expression values were normalized to the level at 0.5 dpf ($n = 3$ biologically independent experiments). **c** Semi-quantitative RT-PCR analysis of mRNA expression for *cd248a and cd248b* at different developmental stages and in different adult zebrafish tissues. Data are presented as the mean ± SD.

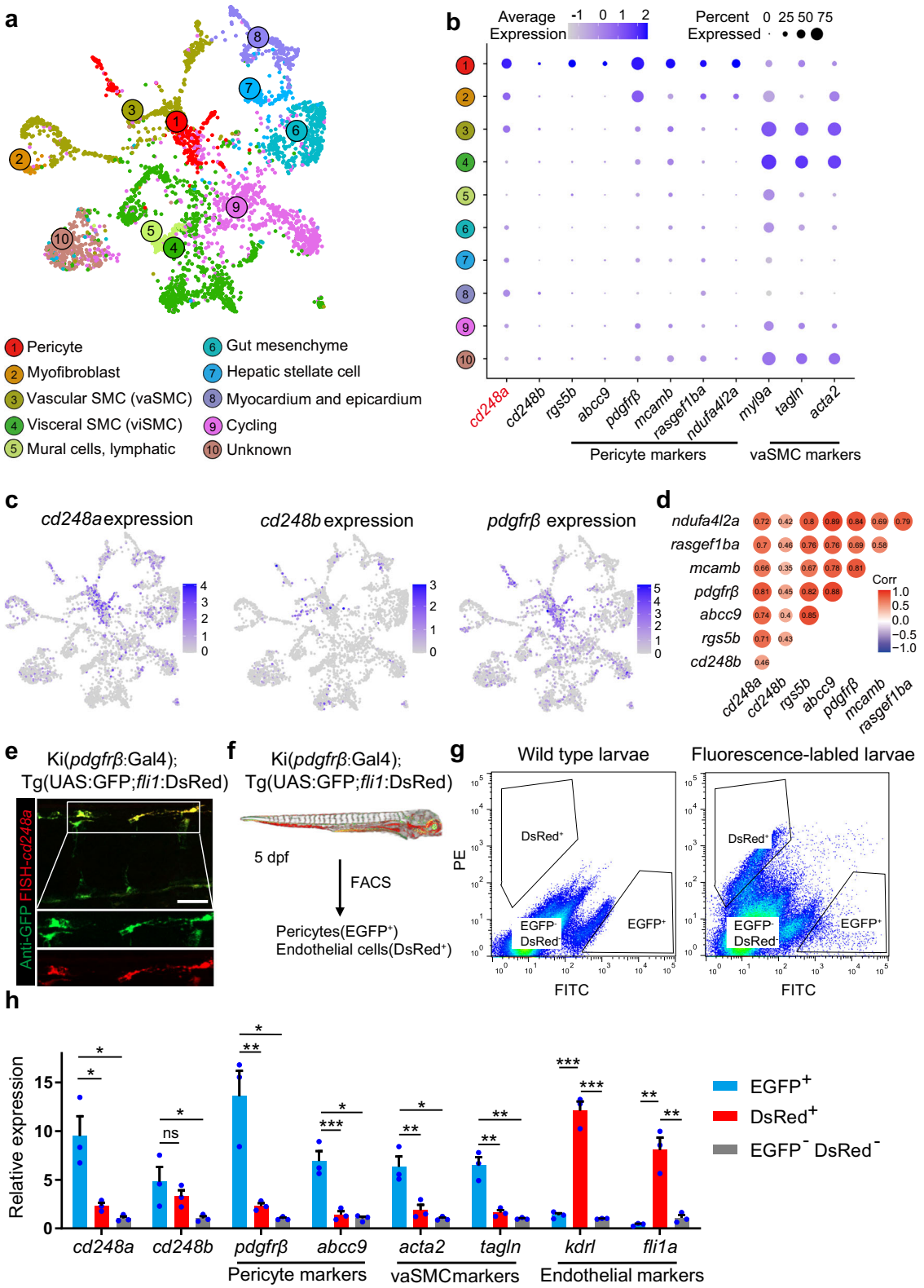

the survival rates of these mutant lines with the WT fish from 1 to 5 dpf and found no significant difference (Fig. 3e). Additionally, we tracked and compared the average body length of the mutants with the WT from 2 to 6 dpf (Fig. 3f) and provided representative images of larvae at 3 dpf and 5 dpf (Fig. 3g). While *cd248a*$^{cc11/cc11}$ and *cd248b*$^{cc12/cc12}$ larvae appeared largely similar to wild type, the *cd248a*$^{cc11/cc11}$ larvae exhibited delayed growth and impaired swim bladder development. These findings suggest that although overall development is not severely disrupted in the mutants, specific aspects such as pericyte development and related physiological processes may be compromised in *cd248a* mutants.

We crossed both mutant lines with the Ki(*pdgfrβ*:Gal4) and Tg(UAS:GFP; *fli1*:DsRed) lines to investigate pericyte development by

Fig. 2 | *cd248a* is highly expressed in pericytes. a Using publicly available single-cell sequencing data set (GSE223922), we show a UMAP projection of 3866 non-skeletal muscle cells collected from whole zebrafish embryos at 50 different developmental stages between 14 and 120 hpf. **b** Dot plots showing the expression of *cd248a*, *cd248b*, and selected pericyte and vascular smooth muscle cell (vaSMC) markers in the indicated clusters. The size of the dot corresponds to the percentage of cluster cells expressing the indicated gene. Color intensity reflects the relative mean expression per cell. **c** UMAP plots of gene expression (blue dots) highlight individual cells that express *cd248a*, *cd248b*, and *pdgfrβ*. Darker blue dots indicate higher gene expression, while gray dots indicate no gene expression. **d** Correlation analysis of *cd248a*, *cd248b* and other pericyte marker genes. **e** Labeling of FISH-*cd248a* (shown in red) and anti-GFP (shown in green) in the Tg(*pdgfrβ*:Gal4; UAS:GFP) larvae at 4 dpf. Scale bars = 50 μm. **f** Schematic of the experimental design for sorting pericytes and endothelial cells. **g** Graphed data of representative FACS analysis of $EGFP^+$ and $DsRed^+$ cells from dissociated 5 dpf Tg(*pdgfrβ*:Gal4; UAS:GFP; *fli1*:DsRed) larvae. **h** qRT-PCR analyses of *cd248a*, *cd248b*, pericyte marker genes (*pdgfrβ* and *abcc9*), vaSMC marker genes (*acta2* and *tagln*) and endothelial cell marker genes (*kdrl* and *fli1a*) followed FACS sorting of $EGFP^+$, $DsRed^+$ and double-negative cells. Data were analyzed by One-way ANOVA and presented as mean ± SD ($n = 3$ biologically independent experiments). *, $p < 0.05$. **, $p < 0.01$. ***, $p < 0.001$. ns: no significance.

examining and counting the number of $pdgfr\beta^+$ pericytes. At 3 and 5 dpf, the number of $pdgfr\beta^+$ pericytes in *cd248a* mutant and double mutant larvae was significantly lower than that in wild-type larvae both in the brain (Fig. 4a-d) and trunk (Fig. 4d-g). In contrast, no significant differences were detected in *cd248b* mutant larvae (Fig. 4a-g). To validate this pericyte deficiency, we determined the *pdgfrβ*-positive ratio in 5 dpf larvae using FCAS. The results corroborated the findings from the above confocal analyses (Fig. 4h).

The defective BBB in *cd248a*$^{cc11/cc11}$ zebrafish can be partially rescued by injecting *cd248a* mRNA

Pericytes are crucial for regulating BBB integrity, and their deficiency can increase BBB permeability. To determine whether the defective BBB is due to impaired pericyte coverage resulting from the loss of *cd248a* function, we conducted a dye diffusion assay using Alexa Fluor™-647 cadaverine (1 kDa, 0.5 mg/ml). This assay visualizes and quantifies vascular leakage by measuring the fluorescence intensity of cadaverine in the extravascular space. Our data showed significantly increased vascular permeability in *cd248a*$^{cc11/cc11}$ zebrafish compared to *cd248a*$^{+/+}$ controls (Fig. 5a). To confirm that the increased permeability was indeed caused by *cd248a* deficiency, we performed a rescue experiment by injecting in vitro synthesized *cd248a* or *cd248b* mRNA into zebrafish eggs. The results indicated that only *cd248a* mRNA, but not *cd248b* mRNA, could partially restore the phenotype of *cd248a* mutant larvae (Fig. 5a-c).

Cd248a regulates pericyte proliferation and functions through Pdgfrβ

To investigate whether the increase in pericyte number was due to pericyte proliferation regulated by *cd248a*, EdU staining was used to label proliferating pericytes[26]. Compared with *cd248a*$^{+/+}$ larvae, *cd248a*$^{cc11/cc11}$ zebrafish larvae exhibited significantly fewer pericytes, and the percentage of EdU^+ pericytes (defined as the number of $pdgfr\beta^+$ EdU^+ pericytes divided by the total number of $pdgfr\beta^+$ pericytes) was significantly lower (Fig. 6a, b). Overexpression of *cd248a* increased the number of $pdgfr\beta^+$ pericytes in *cd248a*$^{+/+}$ larvae (Fig. 6c, d, Supplementary Fig. 3a), and restored the pericyte deficiency phenotype in *cd248a*$^{cc11/cc11}$ larvae in both the brain and trunk (Fig. 6e, f, Supplementary Fig. 3b). These results indicate that *cd248a* functions in regulating pericyte proliferation.

Previous data have shown that CD248 is involved in hepatic stellate cell proliferation induced by PDGF-BB stimulation[20] and that Pdgfb/Pdgfrβ signaling is crucial for zebrafish pericyte proliferation[27], suggesting that *cd248a* may regulate pericyte proliferation, at least in part, by regulating Pdgfrβ function. To test this hypothesis, zebrafish embryos were treated with the PDGFRβ inhibitor AG1295, a blocker of mural cell proliferation[10,28]. Figure 6c and d shows that the increase in pericytes caused by overexpression of *cd248a* did not occur when larvae were treated with 25 μM AG1295. Additionally, Overexpressing *pdgfrβ* could restore the pericyte deficiency in *cd248a*$^{cc11/cc11}$ larvae (Fig. 6e, f, Supplementary Fig. 3b). These results indicate that the regulation of pericyte proliferation by *cd248a* is dependent on the function of Pdgfrβ.

Furthermore, no transcriptional changes in *pdgfrβ* were detected in $pdgfr\beta^+$ pericytes sorted from *cd248a*$^{cc11/cc11}$ zebrafish larvae compared with those sorted from *cd248a*$^{+/+}$ larvae (Fig. 6g). This suggests that the increase in pericyte number regulated by *cd248a* requires Pdgfrβ function through a non-transcriptional mechanism. It has been reported that activation of the PDGF/PDGFR signaling pathway is associated with cell proliferation through modulation of PI3K/Akt pathway, which in turn regulates p53, leading to cell cycle arrest[29–31]. We investigated the expression levels of cell cycle arrest-related genes[26] (*tp53*, *cdkn1a*, *mdm2*, and *gadd45aa*), and the results showed that these genes were all upregulated in *cd248a*$^{cc11/cc11}$ larvae (Fig. 6h). This implies that the decrease in pericytes is at least partially related to cell cycle arrest.

Deletion of *cd248a* increases hypoxia-induced apoptosis of pericytes

Previous studies have emphasized that the transcription of CD248 is regulated by a hypoxic microenvironment, which tends to induce apoptosis in most cells[15,32]. However, it remains unclear whether increased expression of CD248 plays a role in resisting apoptosis in pericytes. To investigate this, $CoCl_2$, a classic hypoxia inducer, was applied to induce hypoxic conditions[33].

The expression levels of *cd248a* and *cd248b* were examined in 5 dpf larvae and in different adult zebrafish organs. As shown in Supplementary Fig. 4a, b, an increase in *cd248a* expression was detected both at the juvenile stage and in various organs of the adult fish (except for the heart and muscle) after $CoCl_2$ treatment. In contrast, elevated *cd248b* expression was detected only in the ovary, brain, eye, and intestine (Supplementary Fig. 4c). These results indicate that the hypoxia-induced expression of *cd248a* in zebrafish is similar to that of human CD248. Thus, we explored the potential anti-apoptotic effect of CD248 using *cd248a* mutant model.

To determine whether enhanced cd248a expression confers resistance to $CoCl_2$-induced apoptosis in pericytes and whether this resistance is mediated by a *tp53*-dependent apoptotic response, a *tp53* morpholino (MO)[34] was injected into *cd248a*$^{cc11/cc11}$ eggs to block the translation of Tp53. TUNEL staining was then performed on 4 dpf larvae exposed to $CoCl_2$ for 24 h. As expected, the number of apoptotic pericytes significantly increased in *cd248a*$^{cc11/cc11}$ larvae after exposure to $CoCl_2$, but only slightly increased in *cd248a*$^{+/+}$ larvae. Knockdown of *tp53* rescued the pericyte apoptotic phenotype (Fig. 7a-c). Notably, *cd248a*$^{cc11/cc11}$ larvae had significantly more apoptotic pericytes than wild-type larvae even without exposure to $CoCl_2$ (Fig. 7a-c). These data indicate that *cd248a* deficiency increases hypoxia-induced pericyte apoptosis through a *tp53*-dependent apoptotic response.

To confirm the protective effect of *cd248a* on pericytes against hypoxia-induced apoptosis, the expression levels of several apoptosis-related genes[35] were analyzed in $pdgfr\beta^+$ pericytes sorted from *cd248a*$^{+/+}$ or *cd248a*$^{cc11/cc11}$ larvae treated with or without $CoCl_2$. Consistent with the TUNEL results, exposure to $CoCl_2$ led to a significant increase in the expression of *caspase3*, *caspase9*, *tp53*, and *bax* in *cd248a*-deficient larvae compared to the wild-type group. (Fig. 7f). Overall, these data suggest that *cd248a* alleviates hypoxia-induced pericyte apoptosis by regulating the expression of genes related to the *tp53*-mediated apoptotic signaling pathway.

Discussion

CD248 is a cell membrane protein that is highly expressed in pericytes and fibroblasts during embryogenesis and tumorigenesis. Although CD248 has been extensively studied for its role in tumor neovascularization[13], vessel

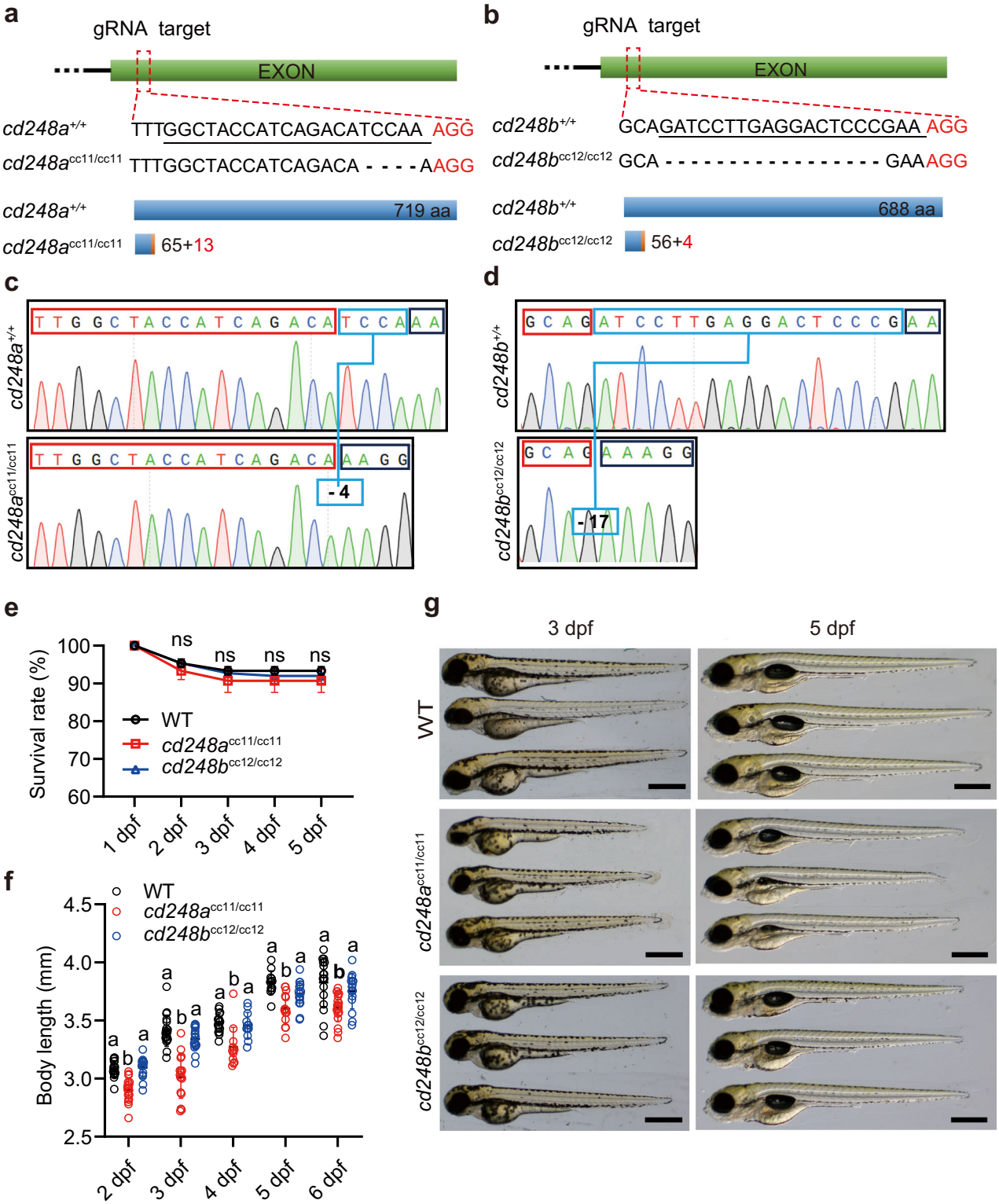

Fig. 3 | Knockouts of *cd248a* and *cd248b* genes in zebrafish using CRISPR/Cas9 system. Diagrams depicting the complete gene structures and deletion mutants of *cd248a* (**a**) and *cd248b* (**b**). The sgRNA target sequence is underlined. The wild-type Cd248a protein consists of 719 amino acids; the Cd248a mutant (*cd248a*$^{cc11/cc11}$) consists of only 65 amino acids identical to the wild type and 13 frameshifted amino acids. The wild type Cd248b protein consists of 668 amino acids; the Cd248b mutant (*cd248b*$^{cc12/cc12}$) consists of only 56 amino acids identical to wild type and 4 frame-shifted amino acids. Sequencing analysis shows indels sites in *cd248a*$^{cc11/cc11}$ (**c**) and *cd248b*$^{cc12/cc12}$ (**d**), indicated with the blue box. **e** Survival rate of *cd248a*$^{cc11/cc11}$, *cd248b*$^{cc12/cc12}$ and wild type zebrafish from 1 to 5 dpf ($n = 3$ biologically independent experiments). **f** Body length of *cd248a*$^{cc11/cc11}$, *cd248b*$^{cc12/cc12}$ and wild-type zebrafish from 2 to 6 dpf ($n \geq 12$ embryos or larvae). **g** Representative images of *cd248a*$^{cc11/cc11}$, *cd248b*$^{cc12/cc12}$ and wild-type larvae at 3 dpf and 5 dpf. Scale bars = 500 μm. Data were analyzed using two-way ANOVA and presented as mean ± SD. ns: no significance. Different alphabets (a and b) between groups indicate significant differences ($p < 0.05$).

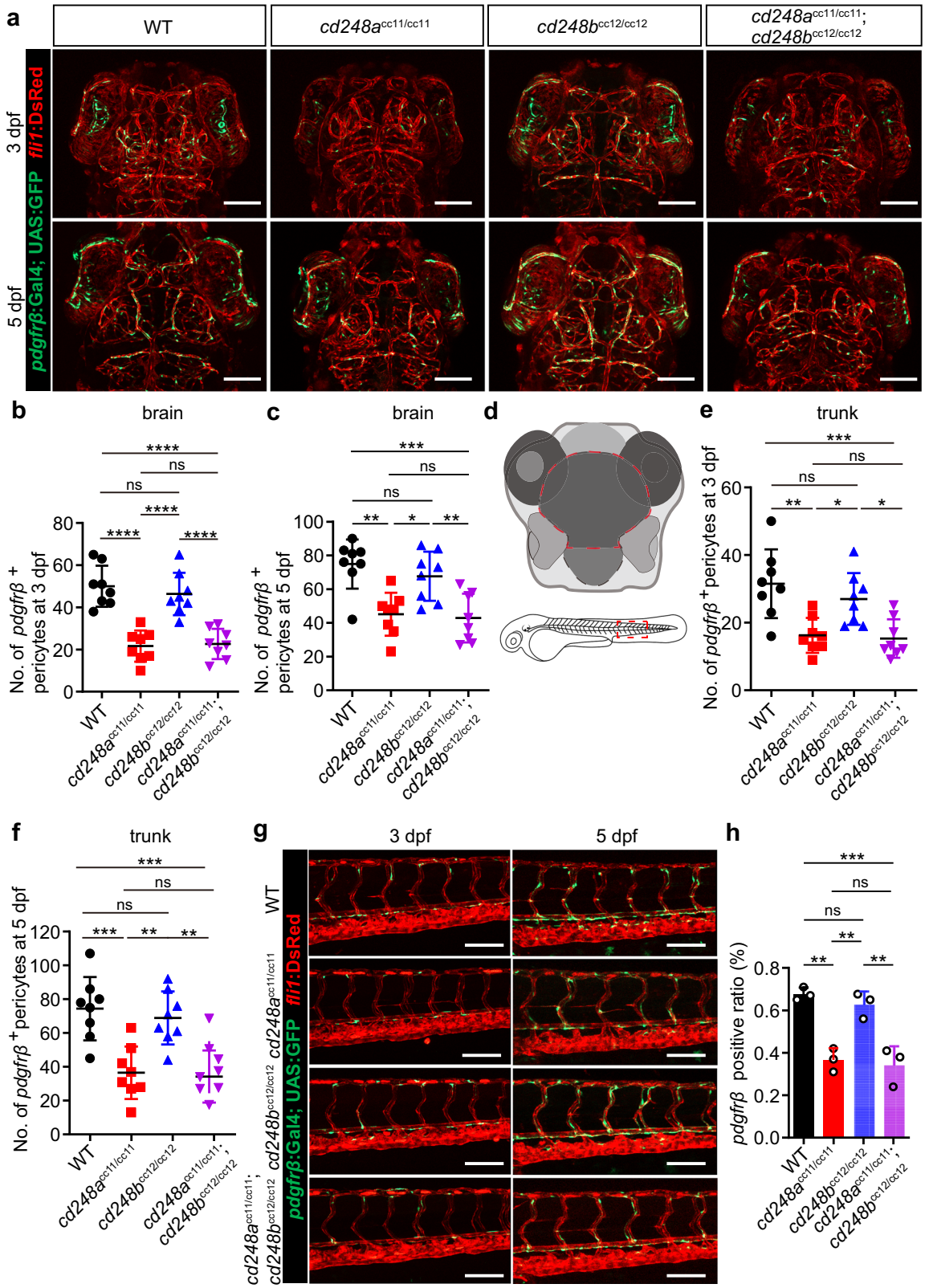

Fig. 4 | Deficit of pericytes in *cd248a* mutant zebrafish. Confocal micrograph (**a**) and quantification of *pdgfrβ*$^{+}$ brain pericytes at 3 dpf (**b**) and 5 dpf (**c**) in wild-type (WT) and mutant zebrafish ($n = 8$ embryos or larvae). Scale bars = 100 μm. **d** Schematic diagram of the counting region, as circled by the red dashed lines. Confocal micrograph (**g**) and quantification of *pdgfrβ*$^{+}$ pericytes in the trunk region at 3 dpf (**e**) and 5 dpf (**f**) in wild-type (WT) and mutant zebrafish ($n = 8$ embryos or larvae). Scale bars = 100 μm. **h** FACS analysis of the proportion of *pdgfrβ*$^{+}$ cells in wild-type and mutant fishes ($n = 3$ biologically independent experiments). Data were analyzed by One-way ANOVA and presented as mean ± SD. *, $p < 0.05$. **, $p < 0.01$. ***, $p < 0.001$.****, $p < 0.0001$. ns: no significance.

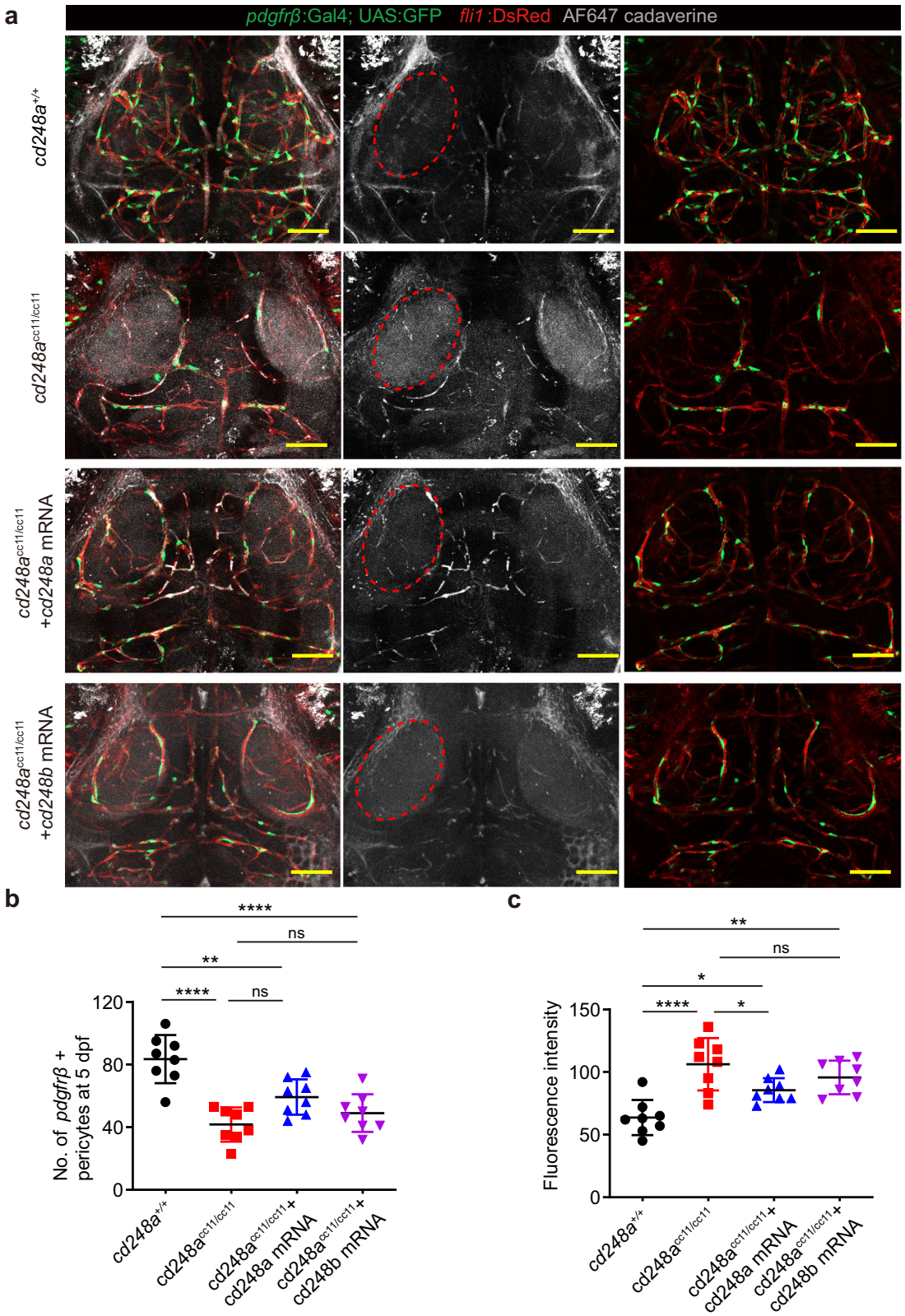

Fig. 5 | The defective BBB in *cd248a*$^{cc11/cc11}$ zebrafish can be rescued by *cd248a* mRNA. a Cerebrovascular images showing infiltration of cadaverine in the extravascular space, as indicated by red circle. Scale bar = 50 μm. **b** Quantification of *pdgfrβ*$^{+}$ brain pericytes in *cd248a*$^{+/+}$ and *cd248a*$^{cc11/cc11}$ larvae with or without mRNA injection ($n = 8$ larvae). **c** Quantitative analysis of fluorescence intensity within the red circle area ($n = 8$ larvae). Data were analyzed by One-way ANOVA and presented as mean ± SD. *, $p < 0.05$. **, $p < 0.01$. ****, $p < 0.0001$. ns: no significance.

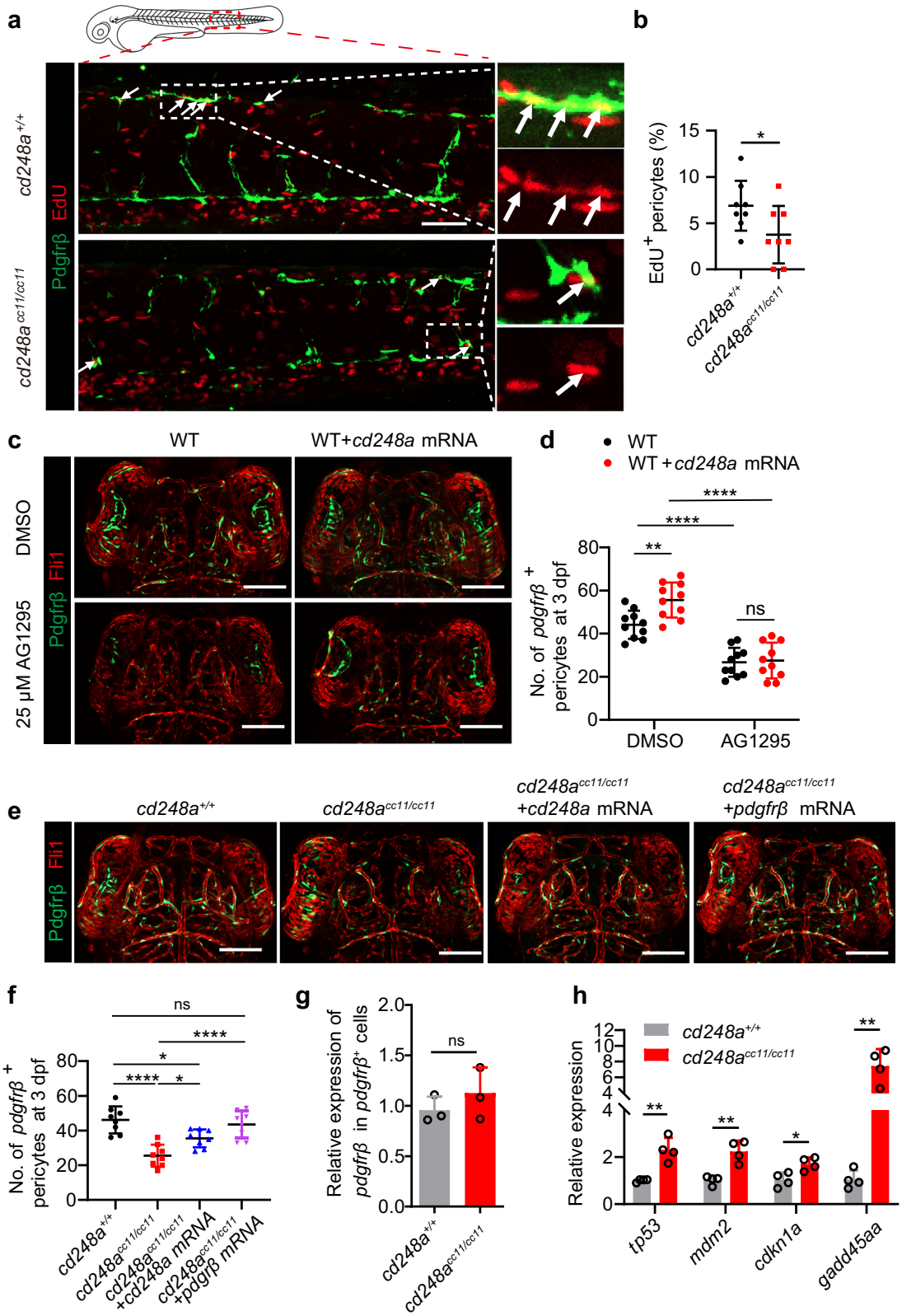

regression[18], wound healing[17], chronic liver injury[20], renal fibrosis[36], and other diseases[37,38], little is known about its role in regulating pericyte proliferation and survival. The zebrafish embryo is an ideal in vivo model for vascular biology research due to its genetic manipulability and optical transparency. To our knowledge, current reports on the role of *cd248a* in pericytes in zebrafish model are still quite limited.

In this study, we revealed that *cd248a* is highly expressed in developing embryos but is weakly expressed in most normal adult organs, except for the heart and kidney tissues. This is consistent with findings in humans and mice, where Cd248 expression persists only in the lung, kidney, and uterus postnatally[39,40]. However, the other paralog, *cd248b*, remains expressed in most adult organs. We further confirmed that *cd248a* is specifically

Fig. 6 | *cd248a* regulates pericyte proliferation in a Pdgfrβ function-dependent manner. a Confocal micrograph showing pericytes (*pdgfrβ*$^{+}$ cells, green) and EdU staining (red) in *cd248a*$^{+/+}$ and *cd248a*$^{cc11/cc11}$ larvae. Arrows indicate EdU-positive pericytes. Scale bar = 50 μm. **b** Quantification of the percentage of EdU-positive pericytes at 3 dpf, represented as the ratio of the number of EdU-positive pericytes to the total number of pericytes within the imaging area ($n = 8$ embryos). Confocal micrograph (**c**) and quantification (**d**) of brain pericytes at 3 dpf in WT and *cd248a*-overexpressing groups with or without exposure to AG1295 ($n = 10$ embryos). Scale bar = 100 μm. Confocal micrograph (**e**) and quantification (**f**) of brain pericytes at 3 dpf in *cd248a*$^{+/+}$ and *cd248a*$^{cc11/cc11}$ groups with or without mRNA injection ($n = 8$ embryos). Scale bar = 100 μm. **g** Relative expression levels of *pdgfrβ* in *pdgfrβ*$^{+}$ cells isolated from *cd248a*$^{+/+}$ and *cd248a*$^{cc11/cc11}$ larvae ($n = 3$ biologically independent experiments). **h** Relative expression levels of cell cycle arrest-related genes in pericytes isolated from *cd248a*$^{+/+}$ and *cd248a*$^{cc11/cc11}$ larvae ($n = 4$ biologically independent experiments). Data in all quantitative panels are presented as mean ± SD; two-tailed unpaired t test (**b**, **g**, **h**), one-way ANOVA (**f**) and two-way ANOVA (**d**). *, $p < 0.05$. **, $p < 0.01$. ****, $p < 0.0001$. ns: no significance.

expressed in pericytes at a higher rate and in a greater proportion than *cd248b*, resulting in expression patterns similar to those of *pdgfrβ*, a typical pericyte marker. Our findings align with previous scRNA-seq analysis, which also identified CD248a as being associated with *pdgfrβ*$^{+}$ pericytes[41]. In summary, these results indicated that *cd248a* could be a pericyte marker gene during the embryonic development of zebrafish.

To further explore the functions of the two *cd248* paralogs in pericyte development, knockout zebrafish lines were generated using the CRISPR/Cas9 system and crossed with the Ki(*pdgfrβ*:Gal4) and Tg(UAS:GFP; *fli1*:DsRed) lines[42]. Compared with wild-type zebrafish, *cd248a* mutant zebrafish presented a deficit of pericytes during embryonic development, similar to the phenotype observed in tumor transplantation models, which have a lower density of pericytes in Cd248-deficient mice[19]. Double-mutant larvae did not exhibit a more severe pericyte deficiency, implying that only *cd248a* plays a vital role in pericyte development. The function of *cd248b* should be explored in future studies. We next characterized the BBB function of *cd248a* mutant larvae with a reduced pericyte population. Consistent with previous findings that pericytes are required for BBB formation and function[43,44], *cd248a* mutant larvae presented a leaky BBB, but no brain hemorrhage was detected in our study. Taken together, these observations indicate that *cd248a* may function to accelerate pericyte proliferation to support intense angiogenesis in developing embryos or tumors.

To test whether *cd248a* promotes pericyte proliferation, we examined EdU incorporation in both wild-type and *cd248a* mutant larvae. The number of EdU^{+} pericytes was significantly lower in *cd248a* knockout larvae than in wild-type control larvae. Conversely, *cd248a* overexpression in wild-type zebrafish resulted in an increase in *pdgfrβ*$^{+}$ pericytes. However, the increase was inhibited when the zebrafish larvae were treated with AG1295, a pharmacological Pdgfrβ inhibitor, suggesting that Pdgfrβ function is required for *cd248a* to regulate pericyte proliferation. Another finding that overexpressing *pdgfrβ* could restore the pericyte deficiency phenotype further supports this viewpoint. Previous work has shown that the Pdgfrb expression level is an intrinsic determinant of pericyte proliferation rate[27,44], but we did not detect a change in *pdgfrb* expression in individual pericytes isolated from *cd248a* mutants and wild-type larvae. This is consistent with a Cd248 knockout mouse model in which the PDGFRβ expression levels in hepatic stellate cells are similar to those in wild-type controls, yet their proliferation could not be induced by PDGF-BB stimulation[20]. These results suggest that *cd248a* may regulate Pdgfrb functions through a non-transcriptional mechanism, likely involving the activation of downstream signaling pathways. It has been reported that the PI3K/Akt pathway, activated by PDGF/PDGFR signaling, is associated with cell proliferation, which mediates the regulation of p53, leading to cell cycle arrest[29–31]. Our findings of elevated expression of cell cycle arrest-related genes in *cd248a*$^{cc11/cc11}$ larvae confirmed this inference. Given the limitations of protein detection in the zebrafish pericyte model, further work is needed to explore this mechanism in greater depth in pericyte cell lines.

Another important function of *cd248a* in pericytes was documented in our work. We found that *cd248a* expression is increased under hypoxic conditions, consistent with previous reports that the transcription of CD248 is regulated by HIF-2[15]. However, the reason for the upregulation of *cd248a* in the hypoxic microenvironment is still unclear. In our study, the increase in the number of apoptotic pericytes in *cd248a* mutant larvae after exposure to $CoCl_2$ was greater than that in the wild-type controls, and this increase could be rescued by injection of *tp53* MO. Our results indicated that *cd248a* deficiency increases hypoxia-induced pericyte apoptosis in a *tp53*-dependent manner. Although the function of p53 in mediating apoptosis under hypoxia has been extensively investigated[45,46], how *cd248a* regulates *tp53* under hypoxia remains unclear.

Furthermore, we found that the expression levels of *tp53*, *tp53* target gene (*bax*) and other proapoptotic genes (*caspase3* and *caspase9*) in *cd248a* mutants were significantly increased after $CoCl_2$ exposure. In contrast, in the wild-type zebrafish, the expression levels of most genes did not change significantly. These results indicate that *cd248a* plays a crucial role in resisting hypoxia-induced apoptosis in pericytes, depending on the regulation of *tp53*.

In summary, this study investigated the functions of the *cd248a* and *cd248b* genes in zebrafish pericytes. In contrast to *cd248b*, *cd248a* appears to be more likely expressed in pericytes. Furthermore, *cd248a* promoted the expansion of pericytes, possibly by regulating Pdgfrb function. Additionally, *cd248a* is clearly involved in increasing pericyte resistance to hypoxia-induced apoptosis in a *tp53*-dependent manner, but the precise regulatory mechanisms of *cd248a* remain to be identified.

Methods

Ethical approval

The animal experiment was conducted according to the "Guide for the Care and Use of Laboratory Animals" (Eighth Edition, 2011) and has been approved by the Laboratory Animal Welfare and Ethics Committee of the Third Military Medical University (Approval ID: AMUWE20223877).

Zebrafish culture

All fish were raised in an automatic water cycler system at 28.5 °C on a 14/10 h daily light cycle, and fed newly hatched brine shrimp twice each day. Embryos were maintained in E3 water. The transgenic lines Ki(*pdgfrβ*:Gal4) and Tg(UAS:GFP; *fli1*:DsRed) were used in this study to visualize pericytes and endothelial cells, respectively. These lines have been characterized by Bing et al.[42].

Generation of the *cd248a* and *cd248b* mutant zebrafish

cd248a or *cd248b* in zebrafish was disrupted according to a standardized gene knockout protocol using CRISPR/Cas9 technique[47]. Briefly, target sites of *cd248a* and *cd248b* were designed using an online tool available at http://chopchop.cbu.uib.no. sgRNAs transcription templates were generated through PCR with T7-targetsite-F primers and a universal reverse primer gRNA-R (Supplementary Table 1). The sgRNAs and Cas9 capped mRNA were synthesized in vitro with a MAXIscript T7 Kit (Invitrogen, AM1314M) and Ambion mMESSAGE mMACHINE T7 Transcription Kit (Invitrogen, AM1344), respectively. Then, Cas9-capped mRNA (300 ng/μL) and sgRNA (30 ng/μl) were co-injected into zebrafish embryos at the single-cell stage. The T7E1 assay was performed to detect the efficiency using PCR product of genomic DNA from injected embryos at 48 hpf.

Whole-mount fluorescence in situ hybridization and antibody staining

Combined whole-mount fluorescence in situ hybridization and antibody staining in Tg(*pdgfrβ*:Gal4; UAS:GFP) zebrafish larvae was performed according to published protocols[48]. The fragment of *cd248a* was generated through PCR using the following primers: *cd248a* forward, 5′-CCCTCTTGACTTCCCTGGAG -3′; T7-*cd248a* reverse, 5′- TAATACGA

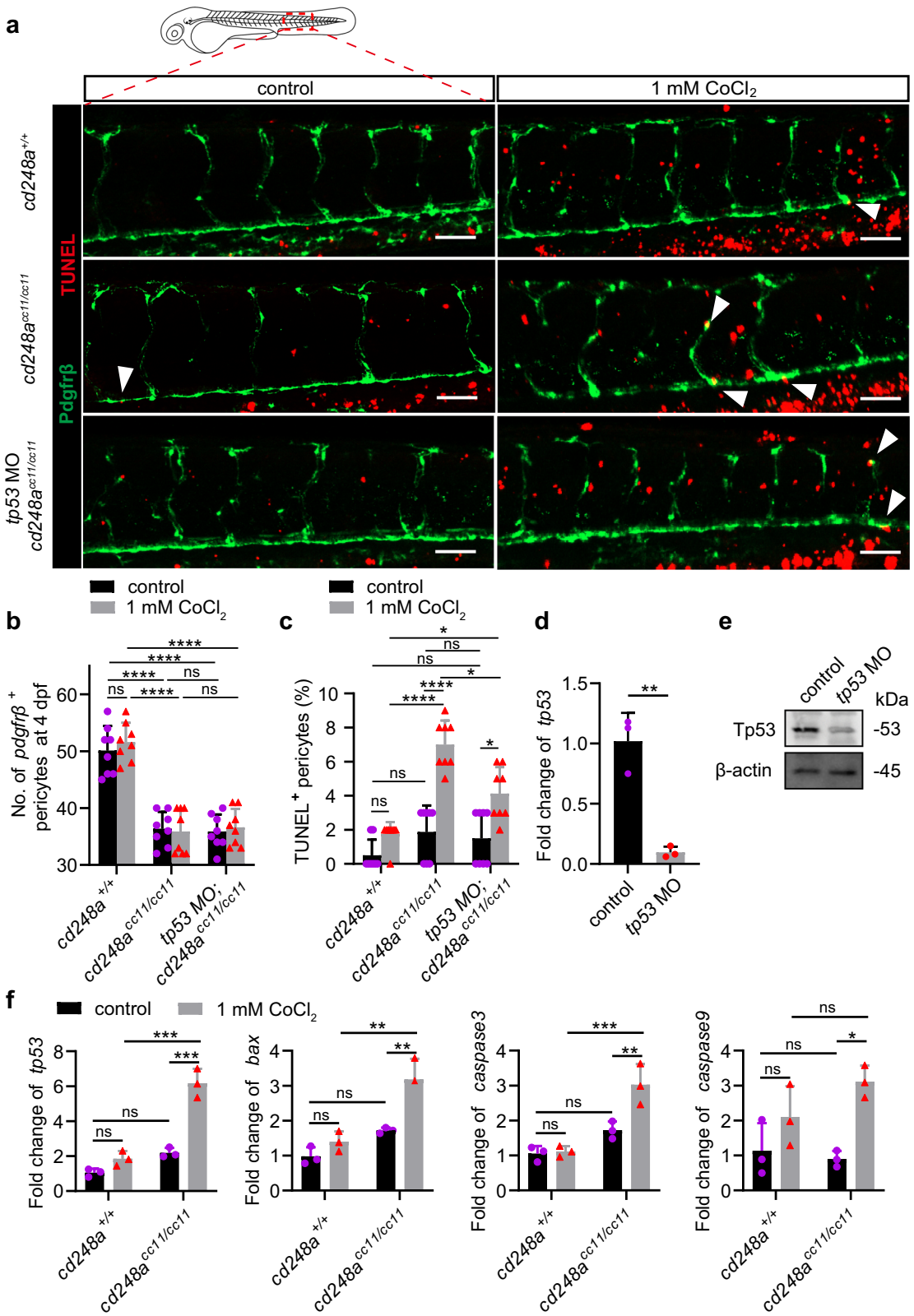

Fig. 7 | Deletion of *cd248a* increases hypoxia-induced apoptosis. a Confocal micrograph showing pericytes (*pdgfrβ*$^{+}$ cells, green) and TUNEL staining (red) in WT and *cd248a*$^{cc11/cc11}$ larvae with or without *tp53* MO injection at 4 dpf. Arrows indicate TUNEL-positive pericytes. Scale bar = 50 μm. **b** Quantification of pericyte numbers in WT and *cd248a*$^{cc11/cc11}$ larvae with or without *tp53* MO injection at 4 dpf within the imaging area ($n = 8$ larvae). **c** Quantification of the percentage of TUNEL-positive pericytes at 4 dpf represented as a ratio of the TUNEL-positive pericyte to the total number of pericytes within the imaging area ($n = 8$ larvae). The effectiveness of the *tp53* MO in blocking transcription (**d**) and translation (**e**) ($n = 3$ biologically independent experiments). **f** Relative expression levels of apoptosis-related genes in pericytes isolated from *cd248a*$^{+/+}$ and *cd248a*$^{cc11/cc11}$ larvae with or without exposure to $CoCl_2$ ($n = 3$ biologically independent experiments). Data in all quantitative panels are presented as mean ± SD; two-tailed unpaired t test (**d**), and two-way ANOVA (**b**, **c** and **f**). *, $p < 0.05$. **, $p < 0.01$. ***, $p < 0.001$. ****, $p < 0.0001$. ns: no significance.

CTCACTATAGGGCAAGCTGTCTTGTTTGCCAT -3′. *cd248a* antisense Fluo-labeled RNA probe was synthesized in vitro with T7 RNA-polymerase (Roche, cat. no. 10881767001). For the staining, a goat anti-GFP primary antibody (1:300, Invitrogen, PA5-143588) and Alexa-488 donkey anti-goat IgG secondary antibody (1:500, Invitrogen, A-11055) were used.

For TUNEL assays, embryos that had been labeled with a GFP antibody were incubated in 100 µl staining solution (Beyotime, C1089) at 37 °C for 1 h according to the manufacturer's instructions. The embryos were then washed in PBST, mounted, and imaged. For EdU labeling, zebrafish embryos at 3 dpf were treated with 500 µM EdU containing 5% dimethylsulfoxide in embryo medium for 4 h at 28 °C on a shaker. They were then fixed in 4% PFA overnight. The GFP fluorescent was detected as described above, and the EdU labeled cells were detected using BeyoClick™ EDU Cell Proliferation Kit with Alexa Fluor 647 (Beyotime, C0081) according to the manufacturer's instructions.

In vitro mRNA synthesis and mRNA microinjection

The full open reading frame (ORF) of zebrafish *cd248a* (NM_001099228.3), *cd248b* (XM_021469088.2), and *pdgfrβ* (NM_001190933.1) were amplified using the PrimeSTAR Max Premix (Takara, R045Q). The pCS2-*cd248a*, pCS2-*cd248b*, and pCS2-*pdgfrβ* vectors were constructed by inserting their ORF into the EcoRI/SnaBI cloning sites of the pCS2+ vector. Capped mRNAs were then produced using Ambion mMESSAGE Mmachine T7 Transcription Kit (Invitrogen, AM1344). The purified mRNA was injected into the one-cell stage embryos at a concentration of 100 ng/µl. The samples were incubated at 28.5 °C before collection.

MO injection

The *tp53* MO-ATG sequence, 5′-GCGCCATTGCTTTGCAAGAATTG -3′, was obtained from Gene Tools[34] and solubilized in water at a concentration of 1 mM. The *tp53* MO and a control MO were injected into the yolk of one-cell stage embryos at the same volume.

Drug treatment

To inhibit pigmentation, embryos were treated with 0.003% N-phenylthiourea (PTU; Sigma Aldrich, P7629) at 24 hpf. For PDGF receptor inhibitor assays, embryos were treated with 25 µM AG1295(MCE, HY-101957) or an equivalent volume of DMSO in E3 media from 2 dpf to 3 dpf. For hypoxic treatments, embryos were exposed to 0.5 or 1.0 mM $CoCl_2$ (Sigma Aldrich, 31277) from 3 dpf to 4 dpf.

FACS analysis

To dissociate embryos and obtain single-cell suspensions, we followed established protocols with minor modification[49]. We used embryos with Ki(*pdgfrβ*:Gal4) and Tg(UAS:GFP;*fli1*:DsRed) transgenic backgrounds to sort EGFP-positive or DsRed-positive cells, thereby isolating pericytes and endothelial cells. WT or mutant embryos at 5 dpf with EGFP and DsRed fluorescence were disaggregated using the Papain Dissociation System (Worthington Biochemical, LK003150) according to the manufacturer's instructions. The cell suspension was then used to sort out pericytes and ECs using the Beckman coulter Moflo XDP. Our gating strategy involved selecting the target cell population based on Forward Scatter and Side Scatter parameters, with positive cells being identified using negative control profiles as a reference.

Analysis of mRNA expression level

Total RNA was isolated from staged embryos, adult organs, or FACS-sorted zebrafish pericytes and endothelial cells using TRIzol reagent according to the manufacturer's instructions (Fastagen, 220010). The extracted RNA was reverse transcribed using RNA Reverse Transcription kit (TRANSGEN, AE341). Semi-quantitative RT-PCR was performed using EasyTaq PCR SuperMix (TRANSGEN, AS111) in a 20 µL reaction contain 1 µL cDNA, with primers as indicated in Supplementary Table 1. Amplicons were visualized by electrophoresis on a 2% agarose gel using equal volume of PCR product. Quantitative real-time PCR (qPCR) was performed using TransStart Green qPCR SuperMixon (TRANSGEN, AQ101) on a CFX96 Real-Time PCR Detection System (Bio-Rad), following manufacturer's instructions and using primers listed in Supplementary Table 1. The relative expression of selected genes was calculated using the $2^{-\Delta\Delta Ct}$ method with *18 s* as reference.

Western blot analysis

Sixty larvae from each group were collected in a single tube and lysed in a lysis buffer containing protease and phosphatase inhibitors. The following antibodies were used: p53 antibody (1:1000, GeneTex, GTX102965) and β-actin antibody (1:1000, Cell Signaling Technology, 8457). Vilber FUSION FX6 was used to image Western blots.

Measurement of brain vascular integrity

A dye diffusion assay was performed to analyze the integrity of BBB in vivo[33,50]. A volume of 10 nl of Alexa Fluor™-647 cadaverine (1 kDa, 0.5 mg/ml, Invitrogen, A30679) was injected into the blood circulation system of 5 dpf zebrafish larvae via the common cardinal vein. Images of the cerebrovasculature were captured immediately after the injection. The relative fluorescence intensity of the dyes was measured and analyzed by Qupath (v.0.2.3) software.

Imaging and quantification

For confocal imaging, embryos were anesthetized in 0.01% tricaine (Sigma, A5040) and mounted in 1.2% low-melting agarose (Invitrogen, 16520100), and covered with E3 water. Then embryos were imaged on a Zeiss LSM 900 confocal microscope using a 10x objective at a resolution of 1024 × 1024. Z-stacks were acquired in 5-µm increments. Quantification of pericytes in embryonic trunk or brain was performed using Qupath (v.0.2.3).

Statistics and reproducibility

Statistical analysis was performed using GraphPad Prism 8 (GraphPad Software, Inc.). Data are presented as the means ± SD. Statistical significance between different groups of samples was performed by ANOVA or two-tailed Student's *t*-test.

Reporting summary

Further information on research design is available in the Nature Portfolio Reporting Summary linked to this article.

Data availability

All data generated during our study are fully documented in the published article and the supplementary information. The source data behind the graphs in the paper can be found in Supplementary Data 1. Entire gel images and blot results can be found in Supplementary Fig. 5. Further information supporting the findings of this study is available from the corresponding author on reasonable request.

Received: 26 July 2024; Accepted: 3 March 2025;
Published online: 17 March 2025

References

1. Glaser, S. F. et al. Circular RNA circPLOD2 regulates pericyte function by targeting the transcription factor KLF4. *Cell Rep.* **42**, 112824 (2023).
2. Armulik, A., Genové, G. & Betsholtz, C. Pericytes: developmental, physiological, and pathological perspectives, problems, and promises. *Dev. Cell* **21**, 193–215 (2011).
3. Suo, L. et al. METTL3-mediated-N6-methyladenosine modification governs pericyte dysfunction during diabetes-induced retinal vascular complication. *Theranostics* **12**, 277–289 (2022).
4. Kusuhara, S., Fukushima, Y., Ogura, S., Inoue, N. & Uemura, A. Pathophysiology of diabetic retinopathy: the old and the new. *Diab. Metab. J.* **42**, 364–376 (2018).

5. Miners, J. S., Schulz, I. & Love, S. Differing associations between Ab accumulation, hypoperfusion, blood-brain barrier dysfunction and loss of PDGFRB pericyte marker in the precuneus and parietal white matter in Alzheimer's disease. *J. Cerebr. Blood Flow Metab.* **38**, 103–115 (2018).
6. Yang, S. et al. Diverse functions and mechanisms of pericytes in ischemic stroke. *Curr. Neuropharmacol.* **15**, 892–905 (2017).
7. Winkler, E. A. et al. Blood-spinal cord barrier breakdown and pericyte reductions in amyotrophic lateral sclerosis. *Acta Neuropathol.* **125**, 111–120 (2013).
8. Montagne, A. et al. Blood-brain barrier breakdown in the aging human hippocampus. *Neuron* **85**, 296–302 (2015).
9. Gaengel, K., Genove, G., Armulik, A. & Betsholtz, C. Endothelial-mural cell signaling in vascular development and angiogenesis. *Arterioscl. Throm. Vas.* **29**, 630–638 (2009).
10. Wang, Y. Y., Pan, L. Y., Moens, C. B. & Appel, B. Notch3 establishes brain vascular integrity by regulating pericyte number. *Development* **141**, 307–317 (2014).
11. Lei, D. et al. bmp3 is required for integrity of blood brain barrier by promoting pericyte coverage in zebrafish embryos. *Curr. Mol. Med.* **17**, 298–303 (2017).
12. Lamont, R. E. et al. Hedgehog signaling via angiopoietin1 is required for developmental vascular stability. *Mech. Dev.* **127**, 159–168 (2010).
13. Bagley, R. G. et al. Endosialin/TEM 1/CD248 is a pericyte marker of embryonic and tumor neovascularization. *Microvasc. Res.* **76**, 180–188 (2008).
14. Madden, S. L. et al. Vascular gene expression in nonneoplastic and malignant brain. *Am. J. Pathol.* **165**, 601–608 (2004).
15. Ohradanova, A. et al. Hypoxia upregulates expression of human endosialin gene via hypoxia-inducible factor 2. *Br. J. Cancer* **99**, 1348–1356 (2008).
16. Nanda, A. et al. Tumor endothelial marker 1 (Tem1) functions in the growth and progression of abdominal tumors. *Proc. Natl. Acad. Sci. USA* **103**, 3351–3356 (2006).
17. Hong, Y. K. et al. Tumor endothelial marker 1 (TEM1/endosialin/CD248) enhances wound healing by interacting with platelet-derived growth factor receptors. *J. Investig. Dermatol.* **139**, 2204–2214 (2019).
18. Simonavicius, N. et al. Pericytes promote selective vessel regression to regulate vascular patterning. *Blood* **120**, 1516–1527 (2012).
19. Hong, C. L. et al. CD248 Regulates Wnt signaling in pericytes to promote angiogenesis and tumor growth in lung cancer. *Cancer Res.* **82**, 3734–3750 (2022).
20. Wilhelm, A. et al. CD248/endosialin critically regulates hepatic stellate cell proliferation during chronic liver injury via a PDGF-regulated mechanism. *Gut* **65**, 1175–1185 (2016).
21. Lax, S. et al. The pericyte and stromal cell marker CD248 (endosialin) is required for efficient lymph node expansion. *Eur. J. Immunol.* **40**, 1884–1889 (2010).
22. Li, X. P. et al. Cd248a and Cd248b in zebrafish participate in innate immune responses. *Front. Immunol.* **13**, 970626 (2022).
23. Sur, A. et al. Single-cell analysis of shared signatures and transcriptional diversity during zebrafish development[Data set]. *Zenodo* https://doi.org/10.5281/zenodo.10048114 (2023).
24. Lawson, N. D. et al. An improved zebrafish transcriptome annotation for sensitive and comprehensive detection of cell type-specific genes. *Elife* **9**, e55792 (2020).
25. Whitesell, T. R. et al. foxc1 is required for embryonic head vascular smooth muscle differentiation in zebrafish. *Dev. Biol.* **453**, 34–47 (2019).
26. Koltowska, K. et al. The RNA helicase Ddx21 controls Vegfc-driven developmental lymphangiogenesis by balancing endothelial cell ribosome biogenesis and p53 function. *Nat. Cell Biol.* **23**, 1136–1147 (2021).
27. Ando, K. et al. Conserved and context-dependent roles for pdgfrb signaling during zebrafish vascular mural cell development. *Dev. Biol.* **479**, 11–22 (2021).
28. Lim, S. E. et al. HIF1α-induced PDGFRβ signaling promotes developmental HSC production via IL-6 activation. *Exp. Hematol.* **46**, 83–95 (2017).
29. Zou, X. et al. Targeting the PDGF/PDGFR signaling pathway for cancer therapy: a review. *Int. J. Biol. Macromol.* **202**, 539–557 (2022).
30. Xu, Z. J. et al. Both selenium deficiency and excess impair male reproductive system via inducing oxidative stress-activated PI3K/AKT-mediated apoptosis and cell proliferation signaling in testis of mice. *Free Radic. Biol. Med.* **197**, 15–22 (2023).
31. Abraham, A. G. & O'Neill, E. PI3K/Akt-mediated regulation of p53 in cancer. *Biochem. Soc. Trans.* **42**, 798–803 (2014).
32. Monaci, S. et al. Targeting hypoxia signaling pathways in angiogenesis. *Front. Physiol.* **15**, 1408750 (2024).
33. Yang, Z. G. et al. Autophagy alleviates hypoxia-induced blood-brain barrier injury via regulation of CLDN5 (claudin 5). *Autophagy* **17**, 3048–3067 (2021).
34. Espín, R. et al. TNF receptors regulate vascular homeostasis in zebrafish through a caspase-8, caspase-2 and P53 apoptotic program that bypasses caspase-3. *Dis. Model Mech.* **6**, 383–396 (2013).
35. Wang, F., Zheng, F. F. & Liu, F. Effects of triclosan on antioxidant- and apoptosis-related genes expression in the gill and ovary of zebrafish. *Exp. Anim.* **69**, 199–206 (2020).
36. Xu, C. et al. Antibody-drug conjugates targeting CD248(+) myofibroblasts effectively alleviate renal fibrosis in mice. *FASEB J.* **36** (2022).
37. Maia, M. et al. CD248 and its cytoplasmic domain: a therapeutic target for arthritis. *Arthritis Rheum.***62**, 3595–3606 (2010).
38. Smith, S. W. et al. CD248+ stromal cells are associated with progressive chronic kidney disease. *Kidney Int.* **80**, 200–208 (2011).
39. MacFadyen, J., Savage, K., Wienke, D. & Isacke, C. M. Endosialin is expressed on stromal fibroblasts and CNS pericytes in mouse embryos and is downregulated during development. *Gene Expr. Patterns* **7**, 363–369 (2007).
40. Huang, H. P. et al. Gene targeting and expression analysis of mouse Tem1/endosialin using a lacZ reporter. *Gene Expr. Patterns* **11**, 316–326 (2011).
41. Shih, Y. H., Portman, D., Idrizi, F., Grosse, A. & Lawson, N. D. Integrated molecular analysis identifies a conserved pericyte gene signature in zebrafish. *Development* **148**, dev200189 (2021).
42. Xu, B. et al. Neurons secrete miR-132-containing exosomes to regulate brain vascular integrity. *Cell Res.* **27**, 882–897 (2017).
43. Armulik, A. et al. Pericytes regulate the blood-brain barrier. *Nature* **468**, 557–561 (2010).
44. Tallquist, M. D., French, W. J. & Soriano, P. Additive effects of PDGF receptor β signaling pathways in vascular smooth muscle cell development. *PloS Biol.* **1**, 288–299 (2003).
45. Leszczynska, K. B. et al. Hypoxia-induced p53 modulates both apoptosis and radiosensitivity via AKT. *J. Clin. Investig.* **125**, 2385–2398 (2015).
46. Hammond, E. M. & Giaccia, A. J. The role of p53 in hypoxia-induced apoptosis. *Biochem. Biophys. Res Commun.* **331**, 718–725 (2005).
47. Wang, C. et al. Deletion of mstna and mstnb impairs the immune system and affects growth performance in zebrafish. *Fish. Shellfish Immun.* **72**, 572–580 (2018).
48. He, J. B., Mo, D. S., Chen, J. Y. & Luo, L. F. Combined whole-mount fluorescence in situ hybridization and antibody staining in zebrafish embryos and larvae. *Nat. Protoc.* **15**, 3361–3379 (2020).
49. Burroughs-Garcia, J., Hasan, A., Park, G., Borga, C. & Frazer, J. K. Isolating malignant and non-malignant B cells from lck:eGFP zebrafish. *J. Vis. Exp.* (2019).

50. Wang, L. et al. Suppressing STAT3 activity protects the endothelial barrier from VEGF-mediated vascular permeability. *Dis. Model Mech.* **14** (2021).

Acknowledgements
We are grateful to professor Jiulin Du for providing the Ki (*pdgfrβ*: Gal4) and Tg(UAS:GFP; *fli1*:DsRed) lines. This work was supported by the National Natural Science Foundation of China (Nos. 82172808 and 82325041), the Science and Technology Innovation Guidance Special Project for Academicians in Chongqing (No. 2022YSZX-JCX0006CSTB), and Chongqing Natural Science Foundation (No. cstc2020jcyj-msxmX0374).

Author contributions
C.W., Y.S., and Y.-F.P. conceived and designed the experiments. C.W., Y.-M. Z., Y.Z., L.-L. A., C.-H. L., Y.Y., and M.M. performed the experiments. Y.-Y. J., M.L., and L.Y. analyzed the data. C.W. and C.-S.-Y.W. wrote the manuscript, W.-Y. W., Z.-C. H., and Q.L. provided important advice. Y.S. and Y.-F.P. supervised the research project. All authors contributed to the article and approved the submitted version.

Competing interests
The authors declare no competing interest.

Additional information
Supplementary information The online version contains supplementary material available at https://doi.org/10.1038/s42003-025-07873-8.

Correspondence and requests for materials should be addressed to Yu Shi or Yi-Fang Ping.

Peer review information *Communications Biology* thanks Chang-Yi Wu, Zigang Cao, and the other, anonymous, reviewer(s) for their contribution to the peer review of this work. Primary Handling Editor: Christina Karlsson Rosenthal. A peer review file is available.